



**HAL**  
open science

## Niche breadth of Amazonian trees increases with niche optimum across broad edaphic gradients

Jason Vleminckx, Oscar Valverde Barrantes, Claire Fortunel, C. E. Timothy Paine, David Bauman, Julien Engel, Pascal Petronelli, Nállarett Dávila, Marcos Rios, Elvis Harry Valderrama Sandoval, et al.

### ► To cite this version:

Jason Vleminckx, Oscar Valverde Barrantes, Claire Fortunel, C. E. Timothy Paine, David Bauman, et al.. Niche breadth of Amazonian trees increases with niche optimum across broad edaphic gradients. *Ecology*, 2023, 104 (7), pp.e4053. 10.1002/ecy.4053 . hal-04098939

**HAL Id: hal-04098939**

**<https://hal.inrae.fr/hal-04098939>**

Submitted on 26 Oct 2023

**HAL** is a multi-disciplinary open access archive for the deposit and dissemination of scientific research documents, whether they are published or not. The documents may come from teaching and research institutions in France or abroad, or from public or private research centers.

L'archive ouverte pluridisciplinaire **HAL**, est destinée au dépôt et à la diffusion de documents scientifiques de niveau recherche, publiés ou non, émanant des établissements d'enseignement et de recherche français ou étrangers, des laboratoires publics ou privés.

1 1. Title page

2 **Journal name:** *Ecology*

3 **Manuscript type:** *Article*

4 **Title:**

5 Niche breadth of Amazonian trees increases with niche optimum across broad edaphic  
6 gradients.

7 **Author list and affiliation**

8 Jason Vleminckx<sup>1,2,3</sup>, Oscar Valverde Barrantes<sup>2,4</sup>, Claire Fortunel<sup>5</sup>, C.E. Timothy Paine<sup>6</sup>,  
9 David Bauman<sup>5,7</sup>, Julien Engel<sup>4,5</sup>, Pascal Petronelli<sup>8</sup>, Nállarett Dávila<sup>9†</sup>, Marcos Rios<sup>9</sup>, Elvis  
10 Harry Valderrama Sandoval<sup>10</sup>, Italo Mesones<sup>11</sup>, Elodie Allié<sup>8,12</sup>, Jean-Yves Goret<sup>12</sup>, Freddie C.  
11 Draper<sup>13</sup>, Juan Ernesto Guevara Andino<sup>14</sup>, Solène Bérroujon<sup>15</sup>, Paul V. A. Fine<sup>16</sup>, Christopher  
12 Baraloto<sup>2,4,12</sup>

13

14 1. Yale Institute For Biospheric Studies (YIBS), Yale University, New Haven, CT, USA.

15 ORCID: 0000-0001-7557-0866.

16 2. Department of Biological Sciences and Institute of Environment, Florida International Univ.,

17 FL, USA.

18 3. Plant Ecology and Biogeochemistry lab, Faculty of Sciences, Université Libre de Bruxelles,

19 Brussels, Belgium.

20 4. International Center for Tropical Botany, Dept of Biological Sciences, Florida International

21 Univ., Miami, FL, USA.

22 5. AMAP (Botanique et Modélisation de l'Architecture des Plantes et des Végétations),

23 Université de Montpellier, CIRAD, CNRS, INRAE, IRD, Montpellier, France.

24 6. Environmental and Rural Science, Univ. of New England, Armidale, New South Wales,

25 Australia.

† This author is deceased

- 26 7. Environmental Change Institute, School of Geography and the Environment, University of  
27 Oxford, Oxford, UK.
- 28 8. CIRAD, UMR Ecologie des Forêts de Guyane, AgroParisTech, Univ. De Guyane, Univ. Des  
29 Antilles, Kourou Cedex, France.
- 30 9. Instituto de Investigaciones de la Amazonia Peruana, Iquitos, Peru, Avenida José A.  
31 Quiñones km 2.5, Iquitos, Loreto Perú.
- 32 10. Facultad de Ciencias Biológicas, Universidad Nacional de la Amazonía Peruana, Iquitos,  
33 Loreto, Perú.
- 34 11. Department of Integrative Biology and University and Jepson Herbaria, University of  
35 California, Berkeley, 3040 Valley Life Sciences Building 3140, Berkeley, California  
36 94720-3140 USA.
- 37 12. INRAe, UMR Ecologie de Forêts de Guyane, AgroParisTech, CIRAD, INRA, Univ. de  
38 Guyane, Univ. des Antilles, Kourou Cedex, France.
- 39 13. Center for Global Discovery and Conservation Science, Arizona State University, 1001  
40 South McAllister Avenue Tempe, Tempe, Arizona 85287 USA.
- 41 14. Field Museum of Natural History, Chicago, IL, USA. ORCID: 0000-0002-5433-6218.
- 42 15. EcoFoG, UMR Ecologie des Forêts de Guyane, AgroParisTech, Univ. de Guyane, Univ.  
43 des Antilles, Kourou Cedex, France.

44 **Corresponding author:** Jason Vleminckx (email: [jasvlx86@gmail.com](mailto:jasvlx86@gmail.com)).

45 **Open Data Agreement:** Data is available in Vleminckx et al. (2023), provided through the  
46 Harvard Dataverse repository: <https://doi.org/10.7910/DVN/VWAJYR>

47 **Key-words:** abiotic filtering, competitive exclusion, functional traits, Neotropical forests,  
48 niche breadth, niche position, range of resource use, soil nutrient availability, tree community  
49 assembly.

50 2. Abstract

51 Understanding how biotic interactions and environmental filtering mediated by soil  
52 properties shape plant community assembly is a major challenge in ecology, especially when  
53 studying complex and hyper-diverse ecosystems like tropical forests. To shed light on the  
54 influence of both factors, we examined how the edaphic optimum of species (their niche  
55 position) relates to their edaphic range (their niche breadth) along different environmental  
56 gradients, and how this translates into functional strategies.

57 Here we test four scenarios describing the shape of the niche breadth – niche position  
58 relationship, including one neutral scenario and three scenarios proposing different relative  
59 influences of abiotic and biotic factors on community assembly along a soil resource gradient.  
60 To do so, we used soil concentration data for five key nutrients (N, P, Ca, Mg and K), along  
61 with accurate measurements of 14 leaf, stem and root traits for 246 tree species inventoried in  
62 101 plots located across Eastern (French Guiana) and Western (Peru) Amazonia.

63 We found that species niche breadth increased linearly with species niche position along  
64 each soil nutrient gradient. This increase was associated with more resource acquisitive traits  
65 in the leaves and the roots for soil N, Ca, Mg and K concentration, while it was negatively  
66 associated with wood density for soil P concentration. These observations agreed with one of  
67 our hypothetical scenarios in which species with resource conservation traits are confined to  
68 the most nutrient-depleted soils (abiotic filter), but they are outperformed by faster-growing  
69 species on more fertile conditions (biotic filter). Our results refine and strengthen support for  
70 niche theories of species assembly, while providing an integrated approach to improve forest  
71 management policies.

### 72 3. Main text

#### 73 **Introduction**

74 A major interest among plant community and evolutionary biologists is to better  
75 understand how environmental filtering and biotic interactions shape community assembly.  
76 Many studies examining the determinants of plant  $\beta$ -diversity have emphasized the role of  
77 abiotic conditions, such as soil properties, through filtering processes related to species resource  
78 acquisition strategies and tolerance to drought and toxicity (Condit et al. 2013, Kraft et al. 2015,  
79 Vleminckx et al. 2017, Van Breugel et al. 2019). Several theories have suggested that  
80 hyperdiverse communities such as tropical forests also experience strong biotic interactions,  
81 mediated by intense inter-specific competition for resources and enemy attacks (Schemske  
82 2009, Fine 2006, 2013). Over time, these biotic interactions would have resulted in the local  
83 coexistence of species displaying narrower species niches (Dobzhansky 1950, Pianka 1966,  
84 MacArthur 1969).

85 Habitat heterogeneity remains a major determinant of species turn-over in tropical  
86 forests. In the Amazon, for instance, white-sand habitats show extremely nutrient-depleted  
87 conditions that select for species investing into costly but well-defended tissues (e.g. thick  
88 leaves, hard wood), which render these species less competitive on relatively more fertile  
89 conditions (the growth-defense trade-off; Fine et al. 2006, 2010). Species relative investment  
90 in costly tissues should therefore reflect their optimum along a resource availability gradient.  
91 This optimum should correlate well with the range of resource availability a species can  
92 tolerate, under the assumption that poor-soil specialists are poor competitors in fertile  
93 conditions and are thereby confined to more restricted niches than faster-growing, rich-soil  
94 specialists. Therefore, comparing the range and optimum of species along a steep resource  
95 availability gradient would help to determine whether conservative species with a high degree  
96 of specialization for poor soil conditions exhibit narrower niches than acquisitive species that

97 grow faster and are more competitive in fertile soils (assuming that no other processes are  
98 becoming important across a broad gradient in soil fertility). Such a comparison would address  
99 a major concern that most studies may overstate the role of abiotic filtering as a community  
100 assembly rule because they fail to consider the potential influence of biotic processes (Kraft et  
101 al. 2014). Additionally, examining how species range and optimum align with different  
102 functional strategies may help to identify adaptive trade-offs that delimit species' niches.  
103 Despite the rapid accumulation of plant functional trait data from diverse ecosystems, few  
104 studies have attempted to link tree species range, optimum, and functional traits (but see  
105 Treurnicht et al. [2019] for Fynbos plant communities of the Cape Floristic Region).

106         Species niche range and optimum relate to the two fundamental parameters proposed by  
107 Hutchinson in his hypervolume model (1957), which has provided one of the most successful  
108 mechanistic constructs of the ecological niche concept. The niche range is commonly referred  
109 to as “niche breadth”, “niche width”, “niche size”, or “ecological amplitude” (Carscadden et al.  
110 2020). Following the Hutchinson’s concept of the niche, the niche breadth determines the range  
111 of environmental conditions that a species can tolerate and the range of resources that it uses  
112 (the potential, or fundamental niche), a range that in reality is more contracted due to  
113 antagonistic interactions mediated by competition for resources, natural enemies, or dispersal  
114 barriers (the realized, or observed niche) (Malanson, Westman & Yan 1992; McGill et al. 2006;  
115 Kraft et al. 2014). The niche optimum represents the set of environmental conditions where the  
116 fitness of a species is highest, as reflected by growth rate, reproduction success, survival,  
117 population size or distribution range (Sexton et al. 2017). This parameter can be assessed by  
118 calculating the niche position, which can be defined as the average, or median value of an  
119 environmental variable where the species occurs, or sometimes as the marginality of this  
120 average value compared to the community mean (Roughgarden 1974). The niche position is  
121 generally used as a proxy for the niche optimum, since the “true” optimal conditions for a

122 species is generally unknown (as its “true” niche breadth) or only estimated via habitat  
123 suitability models (Zuquim et al. 2019). Most studies examine species distributions across only  
124 a portion of their geographic and environmental ranges (Sheth et al. 2020), with sampling  
125 protocols that are rarely explicitly designed to cover an exhaustive representation of the habitat  
126 heterogeneity occurring within a study area, or to provide an equilibrated sampling effort across  
127 contrasted habitat conditions.

128 We can propose at least four hypothetical scenarios predicting the shape of niche  
129 breadth-position relationships along a gradient of soil nutrient availability (Fig. 1). The  
130 relationship between realized species niche breadth and niche position, as well as with their  
131 traits, can be illustrated using Gaussian-like curves for simplicity, as in the classic resource  
132 utilization model of McArthur (1958) (Fig. 1a), even though actual distributions may follow  
133 other forms (Le Bagousse-Pinguet et al. 2017). These curves can be translated into values  
134 describing the relationship of niche breadth plotted against niche position (Fig. 1b).

135 In the first scenario, species niche breadth varies randomly across species, regardless of  
136 their niche position along a gradient of soil resource availability. This pattern would arise if  
137 species were competitively equivalent on any level of that specific soil resource availability,  
138 i.e. if species edaphic distribution is only driven by stochastic and dispersal processes. In that  
139 sense, this scenario is consistent in its outcome with Hubbell’s neutral theory (2001). In the  
140 second scenario, poor soil resources select for species investing in protection against physical  
141 and biological damages, to the detriment of growth, which would render these species  
142 increasingly less competitive when soil fertility increases. In this case, niche breadth should  
143 increase with niche position, and the strength (slope) of this relationship should reflect how  
144 much the cost of adaptation to nutrient-poor soils restricts the ability of conservative species to  
145 compete with more acquisitive species and establish in more fertile habitats. This scenario is  
146 consistent with previous studies showing that poor-soil specialists exhibit resource conservation

147 strategies (e.g. durable tissues with slow turnover), whereas species preferring more fertile soils  
148 are characterized by resource acquisitive traits (e.g. cheap tissues with high turnover) (Fine et  
149 al. 2006, Pinho et al. 2017, Poorter et al. 2018). Scenario 3 is similar to the second scenario,  
150 except that the soil nutrient is not limiting for any species beyond a certain threshold, above  
151 which the nutrient availability does not impact fitness anymore. Niche breadth therefore tends  
152 to reach a plateau. Such a pattern has rarely been emphasized but see Steidinger (2015) for soil  
153 calcium concentration optimum in Panama, which stabilizes and shows a trend consistent with  
154 scenario 3. In the fourth scenario, the increase of potential niche breadth as soil resource  
155 availability becomes less limiting is counter-balanced by a greater “species packing”, i.e. a  
156 constriction of species’ realized niches (MacArthur 1969) resulting from stronger competition  
157 for resources. In this scenario, niche breadth increases with soil resource availability optima,  
158 up to a certain intermediate level of soil fertility, then decreases as a consequence of species  
159 packing, forming a bell-shaped curve.

160 To further shed light on the goodness-of-fit of each scenario to real species assemblages,  
161 we may also inquire whether niche breadth-position relationships show consistent patterns  
162 along decoupled environmental gradients, and whether the same functional trade-offs align  
163 along each gradient. Environmental axes may covary, or vary independently from each other,  
164 either because they are spatially structured at different spatial scales (e.g. climate vs  
165 microhabitat variables), or in the case of soil properties because they are influenced by different  
166 pedological or biogeochemical processes. For instance, some key soil nutrients like base cation  
167 (e.g. calcium, magnesium, potassium) are known to covary, as their concentrations depend on  
168 common chemical and geological conditions (e.g. soil acidity, nature of the bedrock). Other  
169 soil variables, notably anionic nutrients (e.g.  $\text{PO}_4^{3-}$ ,  $\text{NO}_3^{2-}$ ), may display decoupled spatial  
170 variations, as they undergo different chemical constraints (e.g. P immobilization) or different  
171 biogeochemical processes (e.g. N-fixation, nitrification) (Hedin et al. 2009, Vleminckx et al.



172 [2015, Quesada et al. 2010](#)). Whether we observe similar niche breadth-position relationships  
173 along decoupled environmental dimensions, or whether niche breadth and niche position are  
174 influenced by the same resource use traits along those environmental dimensions, are key  
175 questions to improve our understanding of community assembly mechanisms. However, these  
176 questions remain poorly examined ([Futuyma and Moreno 1988, Sultan et al. 1998, Carscadden  
177 et al. 2020](#)).

178         The “world-wide plant economics spectrum hypothesis” ([Reich 2014](#)) suggests that fast-  
179 slow economics spectra would be consistently observed along decoupled soil fertility gradients,  
180 with resource conservation traits being selected on nutrient-depleted soils in general. Although  
181 some evidence has supported this hypothesis ([Poorter et al. 2018](#)), previous studies have also  
182 shown that tree communities display decoupled trait syndromes across leaf, stem and roots  
183 ([Baraloto et al. 2010, Fortunel et al. 2012, Laughlin 2014, Vleminckx et al. 2021, Asefa et al.  
184 2022](#)). These decoupled wood and leaf economic traits have been shown to respond to similar  
185 fertility gradients in tropical forests ([Fortunel et al 2014, Vleminckx et al. 2021](#)). Yet, to date  
186 there has been no attempt to integrate niche breadth data to examine how individual nutrient  
187 availability gradients potentially determine species edaphic ranges, and whether decoupled  
188 traits align with the same fertility gradients.

189         Here, we address these questions using a unique dataset of 246 tree species inventoried  
190 in 101 plots located across Eastern (French Guiana) and Western (Peru) Amazonia, together  
191 with accurate measurements of 14 leaf, stem and root traits. We first examine whether species  
192 niche breadth and niche position, taken separately, are aligned or decoupled among five soil  
193 nutrient availability gradients (N, P, Ca, Mg and K). Second, we examine how well the four  
194 scenarios presented in Fig. 1 match the observed niche breadth-position relationship along each  
195 soil gradient. We address the following specific questions:

- 196 (1) How are species niche breadth and position associated among the different soil  
197 nutrient gradients?
- 198 (2) How well do our four scenarios (Fig. 1) fit the niche breadth-position relationship?
- 199 (3) Are decoupled niche breadth and position dimensions associated with different plant  
200 functional strategies?

## 201 **Methods**

### 202 **Study areas**

203 We established a nested experimental design with replicated plots in habitats displaying  
204 contrasting soil conditions, characteristic of lowland Amazonian forests – white-sand (WS),  
205 Terra Firme (TF) and seasonally flooded forests (SF) (Fortunel et al. 2014, Baraloto et al. 2021)  
206 – at both regional (c.100 km) and basin-wide (2500 km) distances. A total of 101 0.1-ha plots  
207 were inventoried between 2008 and 2018 in ten subregions of tropical moist forest in French  
208 Guiana (hereafter FG; 63 plots) and between 2008 and 2011 in three subregions in Peru (38  
209 plots) (Fig. 2). French Guiana forests stand on an old Precambrian tableland, with old, highly  
210 weathered and nutrient-depleted soils (Gourlet-Fleury et al. 2004). Mean annual rainfall across  
211 inventory subregions ranges between 2160 and 3130 mm (<http://www.worldclim.com/>) and is  
212 distributed seasonally throughout the year. The wet season stretches from December to July and  
213 is usually interrupted in February or March by a short dry period, while the dry season occurs  
214 from August to November with monthly rainfall never exceeding 100 mm. Mean temperature  
215 oscillates between 23.0 and 26.6°C with low seasonal variation (Gourlet-Fleury et al. 2004).  
216 Elevation among subregions ranged from 42 to 529 m. Forests from the Western Amazon in  
217 Peru cover heterogeneous soil conditions consequent to the combined impact of marine  
218 incursions, the Andean uplift, and the weathering of volcanic sediments (Hoorn et al. 2010).  
219 Mean annual rainfall varies between 2405 and 2750 mm, whereas mean temperature ranges

220 from 26.3°C to 26.7°C (<http://www.worldclim.com/>), and elevation from 95 to 173 m. The  
221 study areas are further detailed in Baraloto et al. (2021).

## 222 **Tree species inventories**

223 Trees were inventoried following a modified version of the Gentry plots proposed by Phillips  
224 et al. (2003) and described by Baraloto et al. (2013). Each plot consisted of ten parallel 50 m-  
225 long transects departing perpendicularly from a main 180 m-long central line, successively in  
226 alternate directions every 20 m along the line (a schematic illustration of a plot is provided in  
227 Appendix S1: Figure S1). All stems with a circumference  $\geq 8$  cm at 1.3 m above the ground  
228 (2.5 cm DBH) were inventoried over a two-meter width along each transect. At least one  
229 individual of every putatively-distinct taxon encountered was collected in the field to create  
230 plot-level voucher collections. In rare cases (0.2% of all stems sampled), no identification was  
231 achieved nor could vouchers be collected due to lack of leaves or obstructed canopies. The plot  
232 level vouchers were meticulously sorted so that independent distinct taxa had at least one  
233 collection in each plot. Further sorting resulted in standardized project type collections for all  
234 distinct taxa which were identified at regional herbaria for the Peru (AMAZ) and French Guiana  
235 (CAY) collections. We then further standardized and resolved vouchers from both these  
236 collections during a five-month period at the herbarium of the Missouri Botanical Garden (MO),  
237 such that any unnamed, putative novel species was compared to other congeners from the other  
238 region (Baraloto et al. 2021). At the end, we provided a full detail of all project vouchers  
239 describing our standardized inventories (vouchers and/or photos are available for loan upon  
240 request). Species diversity was characterized in each subregion using species richness, as well  
241 as the effective number of species expected from 1000 random samplings of 2 individuals to  
242 weight for species abundance (Dauby & Hardy 2011) (Table 1).

243 **Soil data**

244 We collected bulked soil cores at 0–15 cm depth at ten regularly spaced positions along the  
245 central line of the plot (Appendix S1: Figure S1). The ten cores were mixed into a 500 g sample  
246 that was dried to constant mass (at 25°C) and sieved (2 mm mesh). Samples from were shipped  
247 to the University of California, Davis DANR laboratory for physical and chemical analyses (see  
248 [Baraloto et al. 2011](#) for full protocol details). The bioavailability of three base cations (Ca, Mg,  
249 K) and P, and the total soil nitrogen concentration (N) were then quantified for each soil sample,  
250 following a protocol described in details Baraloto et al. (2011). We lack data on other soil  
251 variables like soil pH and soil Al, Mn and Fe concentration to evaluate the impact of soil acidity  
252 and toxicity on species niches. The mean and the standard deviation of each soil variable in  
253 each habitat and each study region (Peru and French Guiana, separately) is shown in Table 2.  
254 The distribution of plot values for each soil variable within each edaphic habitat (SF, TF and  
255 WS), and a test of comparison (Wilcoxon-Mann-Whitney) of these values across habitats for  
256 each soil variable are shown in supplementary information (Appendix S2: Figure S1). As a  
257 complementary information, we also show the projection of plots and soil variables in a  
258 Principal Component Analysis (PCA) (see details in Appendix S3: Figure S1).

259 **Functional trait data**

260 We used data for 14 chemical and morphological traits related to resource use and structural  
261 defense, comprising ten leaf, two stem and two fine root traits: Leaf thickness and toughness,  
262 SLA, Leaf C, N, P, Ca, Mg and K concentration, leaf <sup>13</sup>C, sapwood-specific gravity, trunk bark  
263 thickness, fine root tissue density and fine root specific root length (SRL). The unit and  
264 functional role of each trait, along with additional information on trait sampling locations are  
265 provided as online supplementary information ([Vleminckx et al. 2023](#)). These functional data  
266 were obtained from accurate trait measurements from Peruvian and French Guianan samples  
267 collected for 8345 individuals from 1625 species in 371 genera, 78 families and 26 orders

268 covering the Rosidae, Asteridae and early eudicots (Baraloto et al. 2010, Fortunel et al. 2012,  
269 Vleminckx et al. 2021). Missing trait data ranged from 34.96% for leaf thickness up to 74.17%  
270 for root SRL (see Table S2 in Vleminckx et al. 2021). Missing values were imputed using a  
271 Bayesian hierarchical matrix factorization method (BHMF), based on taxonomic information  
272 and co-variation among traits (Fazayeli et al. 2014; see Vleminckx et al. 2021 for details). All  
273 these traits reflect species economics spectrum potentially associated to soil nutrient availability  
274 levels, or intrinsic water-use efficiency (Leaf  $^{13}\text{C}$ ) (Baraloto et al. 2010).

275

## 276 **Data analysis**

### 277 *Niche breadth and niche position data*

278 Species abundance at the plot level was calculated after weighting each tree by the  
279 logarithm of its basal area, to take into account that later life stages are likely to be more  
280 representative of the influence of habitat conditions on species distributions, whereas the  
281 assembly rules of younger trees can be more stochastic (Vleminckx et al. 2015). We then  
282 calculated the niche breadth and the niche position of each of the 246 species that were present  
283 in at least three subregions (i.e., areas comprising plots), across each of the five soil nutrients  
284 (N, P, Ca, Mg and K). For each soil variable, the niche position of each species corresponded  
285 to the median of the soil variable calculated among plots where the species was found  
286 (weighting each plot according to the abundance of the species). The niche breadth was  
287 calculated as the interquartile range (25-75%) of values for the soil variable. The 25-75% range  
288 was chosen to provide robust niche breadth values that were weakly sensitive to outliers  
289 (Steidinger 2015). Calculations using a 20-80% and a 15-85% range provided highly consistent  
290 results that did not modify our interpretations. Prior to any subsequent analysis, niche breadth  
291 and niche position values were normalized (using a Box-Cox transformation) and standardized  
292 (z-score transformation). We then detrended niche breadth values to remove any potential

293 biased inflation of these values induced by the effects of: (i) the total abundance of each species  
294 across all plots, (ii) the number of subregions and (iii) plots in which each species is present,  
295 and (iv) their regional distribution (i.e. dummy variable columns indicating whether each  
296 species is present in one region, i.e. Western or Eastern Amazon, or both regions). This  
297 detrending was performed by using the residuals of a linear regression of niche breadth against  
298 these effects (see details in Appendix S4).

### 299 *Niche breadth and niche position correlations among soil variables*

300 To specifically address question 1, we performed a PCA on the species niche breadth  
301 values corresponding to the different soil nutrients, and the same PCA for species niche position  
302 values. We then tested whether the Pearson correlations of niche breadth and niche position  
303 among the five soil nutrients were statistically significant. Correlations were considered  
304 significant when they were lower or higher than the 2.5-97.5% quantiles of correlation values  
305 obtained after randomizing each nutrient concentration values at the plot level and recalculating  
306 niche breadth and niche position, while preserving the multi-scale spatial structure of each  
307 nutrient within each study region (Peru and French Guiana), independently. To do so, we used  
308 Moran Spectral Randomization (MSR, [Wagner and Dray 2015](#)), a procedure that allows  
309 considering multiscale spatial autocorrelation structures for any type of quantitative variable,  
310 based on spatially weighted connectivity information among sampling points (i.e. the 101 plots  
311 in our case). This information was obtained from an optimized procedure used to choose a  
312 spatial weighted matrix and select a subset of Moran's eigenvector maps (MEMs, [Dray et al.](#)  
313 [2006](#)), following [Bauman et al. \(2018a,b\)](#), using the R package 'adespatial' ([Dray et al. 2022](#)).  
314 MEMs are spatial eigenvectors that model multi-scale spatial structures in any type of  
315 numerical variable. We tested a minimum spanning tree configuration and a Gabriel's graph to  
316 model connectivity among plots, which have been shown appropriate to accurately modeling  
317 structures even when dealing with nested and irregular sampling designs such as ours ([Bauman](#)

318 [et al. 2018a](#)). The spatial weighted connectivity information from the best MEM model (i.e.,  
319 the eigenvector combination that best described the spatial structures in the soils nutrients'  
320 concentration, based on a forward selection with double stopping criterion) is then used in a  
321 spatially constrained randomization algorithm in the MSR method to reproduce variables that  
322 accurately mimic the observed spatial structures of the randomized variable(s).

323 Species in each PCA graph were also characterized by their affinity for each of the three  
324 habitats, by calculating and testing their indicator value (indval), following Dufrêne & Legendre  
325 (1997). This allowed combining quantitative soil information with qualitative visualization of  
326 three well-defined and contrasted habitats of the Amazon region (white-sand, terra firme and  
327 seasonally flooded).

### 328 *Relationship between niche optimum, niche breadth and traits for each soil nutrient*

329 To address question 2, we plotted the niche breadth of species against their niche  
330 position values, for each soil variable. The linear and non-linear relationships between niche  
331 breadth and niche position were fitted using Bayesian regression models. The posterior  
332 distributions of the slope coefficients of interest were summarized through the median and 95%  
333 posterior credibility interval. The linear and non-linear (quadratic) slope coefficient  
334 distributions were fitted (Bayesian updating) using a quadratic approximation ([McElreath](#)  
335 [2020](#)). The shape of the niche breadth-position associations and the importance of the linear  
336 and quadratic coefficients were used to verify which scenario in Fig. 1 best fits the observed  
337 niche breadth-position relationship, for each soil nutrient. Coefficient values were considered  
338 as clearly positive or negative whenever at least 95% of their posterior mass probability was  
339 positive or negative (i.e., did not encompass zero). Scenarios 2 and 3 predict positive values for  
340 the linear coefficient and non-important values for scenarios 1 and 4. Scenarios 3 and 4 predict  
341 negative values for the quadratic coefficient, while the latter is expected to be non-important  
342 for scenarios 1 and 2.

343 To address question 3, we performed a variation partitioning to quantify, for each soil  
344 variable, the fraction (adjusted  $R^2$ ) of species niche breadth variation explained purely by their  
345 niche position and by their functional traits. We then tested the significance of each fraction by  
346 testing whether the observed fraction (adjusted  $R^2$  values) was higher than 95% of null values  
347 obtained with the MSR method described above. If the observed adjusted  $R^2$  value quantifying  
348 the effect of all traits combined was higher than 95 % of the 4999 adjusted  $R^2$  values obtained  
349 with the MSR procedure, then we performed a forward selection to identify the traits that  
350 significantly explained niche breadth variation (Blanchet et al. 2008).

351 Prior to the variation partitioning, we verified whether niche breadth values were  
352 influenced by phylogeny. Phylogeny was modelled using a matrix of dummy variables  
353 assigning “1” for each species (lines) in their corresponding genus and family (in columns), and  
354 “0” for non-matching taxa. The phylogenetic effect was then tested using a residuals  
355 permutation test (Anderson and Legendre 1999), which showed no significant effect for any  
356 soil variable (Appendix S5: Table S1).

357 All analyses described in the methods were performed in the R statistical environment  
358 (R Development Core Team, 2022). We provide the soil, tree inventory and trait data, along  
359 with our R script in the online repository folder: <https://doi.org/10.7910/DVN/VWAJYR>.  
360 References for the R packages used are detailed in the R code.

## 361 **Results**

### 362 **Correlation of niche breadths and positions among soil variables**

363 The two PCAs performed on niche breadth and niche position values showed highly  
364 consistent patterns of variables’ projection, revealing a strong relationship between these two  
365 niche parameters (Procrustes correlation = 0.587;  $P \leq 0.001$ ; MSR test; Fig. 3). There was a  
366 strong coordination of species niche breadth and position for soil cations (Ca, Mg and K) and  
367 to a lesser extent for N. Increasing niche breadth and position values for N, Ca, Mg and K



368 aligned well with increasingly acquisitive functional traits such as higher leaf N concentration  
369 (Fig. 3). Soil P concentration showed a clear decoupling of niche breadth and position values  
370 compared to the other nutrients (Fig. 3). Species significantly indicative of seasonally flooded  
371 and terra firme habitats displayed significantly higher niche breadth and niche position, as well  
372 as higher leaf N and P concentration for soil N, Ca, Mg and K concentration, compared to white-  
373 sand specialists, (Appendix S6: Figure S1, and Appendix S7: Figure S1; for sample size details,  
374 see Appendix S8: Figure S1). The following analyses examine in more details the relationship  
375 between niche breadth, niche position and functional traits for each soil nutrient.

376

### 377 **Functional strategies associated with niche breadth and position**

378 Species niche breadth was positively associated with niche position for each of the five  
379 soil nutrients (Fig. 4). No clear negative quadratic term was detected for niche position,  
380 indicating that relationships were mostly linear and consistent with scenario 2 (Fig. 1). The  
381 niche breadth-position linear relationship was the strongest for soil Ca concentration ( $R^2$  value  
382 = 45.1%), followed by soil N (40.2%), P (26.2%) and K (18.2%) concentration. The effect of  
383 functional traits on niche breadth nearly entirely co-varied with the effect of niche position. In  
384 other words, we did not observe any trait explaining species niche breadth alone. Niche breadth  
385 and position values were not significantly explained by the genus and family identity of species  
386 for any soil variable ( $R^2 < 1\%$ ; Appendix S5: Table S1).

387 Functional traits contributed to species niche breadth ( $P \leq 0.05$ ; MSR test) for soil N  
388 ( $R^2 = 3.7\%$ ) and Ca (12.4%) concentration, with high niche breadth values for these two soil  
389 nutrients being associated with more resource acquisitive strategies among species, in particular  
390 higher SLA, Leaf N and Ca concentrations, and higher fine root SRL (Fig. 4). The Pearson  
391 correlations between each individual trait and species niche breadth for soil N, Ca, Mg and P  
392 concentration are shown in supplementary material (Appendix S9: Figure S1). Species niche

393 breadth for soil K concentration was not significantly explained by functional traits (Fig. 4).  
394 Results obtained with soil Mg concentration were consistent with the ones obtained with soil  
395 Ca concentration (Appendix S10: Figure S1). Functional traits less clearly explained the niche  
396 breadth of soil P ( $R^2=1.9\%$ ), although sapwood density was retained by the forward selection  
397 procedure, with species distributed on the most P-depleted soils showing denser wood than on  
398 less P-limiting conditions.

## 399 **Discussion**

400 Niche properties, characterized by species range (niche breadth) and optimum (niche position)  
401 along soil nutrient gradients, were coordinated among soil N, Ca, Mg and K, but not soil P  
402 (Fig. 3). The decoupling of species niches between soil P concentration and the other nutrients  
403 was associated with different functional strategies (Fig. 4). Our results suggest that species  
404 undergo increasing abiotic constraints that favor costly resource conservation strategies when  
405 soil fertility decreases. These abiotic constraints decrease with increasing soil fertility,  
406 allowing species exhibiting more resource acquisitive traits to occupy increasingly larger  
407 niches, in line with scenario 2 (Fig. 1).

### 408 **Costly poor-soil adaptations limit species edaphic ranges**

409 We found a strong positive and linear increase of species niche breadth with their niche  
410 position, for each soil nutrient (Fig. 3, 4), in contrast with predictions from scenario 1. The  
411 quadratic term of the niche breadth-position relationship was never clearly different from zero  
412 and always positive, which invalidated scenarios 3 and 4 and provided support for scenario 2.  
413 Although our sampling may not have captured the full edaphic distribution for every species,  
414 the gradients that we measured and the care with which we effected taxonomic determinations,  
415 represent a nearly complete picture for most of these species' distributions (Quesada et al. 2010,  
416 Baraloto et al. 2021), such that additional sampling would be unlikely to change the present  
417 results. It is also worth noting that the way we accounted for spatial distribution disparities

418 among species in the analyses strongly limited the potential influences of spatial biases related  
419 to the statistical design (Taylor 1961).

420 Species distributed on the most N and Ca-depleted soils had lower leaf nutrient  
421 concentrations, in particular N and Ca, while also showing relatively low SLA (Fig. 4,  
422 Appendix S7: Figure S1), indicating resource conservation strategies (Fortunel et al. 2014).  
423 These species also displayed relatively low niche breadth values, which may suggest that their  
424 resource conservation traits confine them to these poor soil conditions (generally white-sands),  
425 and exclude them from the more fertile terra firme and seasonally flooded soils.

426 The positive association between species niche breadth for soil Ca concentration and  
427 SRL may reflect the existence of a fast-slow trade-off associated with soil fertility conditions,  
428 with poor soils occupied by species investing in longer roots with lower tissue quality, possibly  
429 associated with higher uptake capacity in more competitive environments. Our results may  
430 suggest that soil Ca limitation has had more influence than the four other soil nutrients studied  
431 here on fine root evolutionary history and is consistent with previous manipulative studies in  
432 tropical Amazonian forests (Wurzburger & Wright 2015). Nevertheless, root traits were  
433 generally poor predictors of niche breadth, possibly because of the multiple alternatives that  
434 plants use for nutrient capture, including investments in mycorrhizal associations, that make  
435 possible a wide spectrum of trait syndromes in the same soil conditions (Valverde-Barrantes et  
436 al. 2017).

437 The niche breadth-position relationship was significantly positive but relatively weaker  
438 for soil K concentration ( $R^2 = 18.2\%$ ) than for soil Ca, N and P concentration ( $\geq 26.2\%$ ; Fig.  
439 4). Yet, niche position and niche breadth for soil K concentration did not show any significant  
440 association with any functional trait, contrary to the three other soil nutrients. Thus, while our  
441 results suggest that K may indeed limit primary productivity, which is consistent with previous  
442 studies in lowland tropical forests (Wright et al. 2011, Baribault et al. 2012, Santiago et al.

443 [2012](#)), they also nuance the idea that single functional traits reflect edaphic adaptations among  
444 tree species. The decoupling of fast-slow economic spectra reported among Amazonian tree  
445 communities ([Baraloto et al. 2010](#), [Fortunel et al. 2012](#), [Vleminckx et al. 2021](#)) may partly  
446 introduce statistical noise when testing a signal between a single trait and a soil variable, and  
447 thus partly explains the weak predictive power of traits on species niche breadth.

448         The marked niche breadth-position relationship observed for soil P ( $R^2 = 26.2\%$ ) was  
449 highly decoupled from the other four soil nutrients (Fig. 3, 4). This pattern was consistent with  
450 the orthogonality between soil P variation and the four other soil nutrients (Appendix S3: Figure  
451 S1). This orthogonality supports previous evidence that soil P availability often varies  
452 independently from cationic nutrients (Ca, Mg, K) or can even be higher on cation-poor sandy  
453 soils, due to the immobilization of P into Al oxyhydroxide complex forms in more fertile,  
454 clayey tropical soils ([Walker & Syers 1976](#), [Vleminckx et al. 2015](#), [Turner 2018](#), [Cunha et al.](#)  
455 [2022](#)). In fact, P availability was even higher on white-sand forests than on the other edaphic  
456 habitats in Peru (Table 2), whereas the reverse pattern was observed in French Guiana. Yet, the  
457 overall niche breadth-position correlation remained strongly positive, even when considering  
458 the disparities of habitat differences for P availability across regions.

459         The decoupling of niche dimensions between soil P and the other four soil nutrients was  
460 associated with different functional dimensions. More specifically, species preferences for terra  
461 firme and seasonally flooded soils, which contained the highest soil N and cation  
462 concentrations, were mostly reflected by acquisitive traits in the leaves, whereas species whose  
463 optimum was on low P availability soils tended to have denser wood. The latter signal was  
464 weak but nevertheless significant (Fig. 4), and while further studies are needed to verify  
465 consistent patterns, it may partly explain the decoupling of traits that has previously been  
466 reported among leaf and woody aboveground organs when measured across broad edaphic  
467 gradients ([Baraloto et al. 2010](#), [Fortunel et al. 2014](#), [Vleminckx et al. 2021](#)).

468 In parallel with using combinations of forward-selected traits in the variation  
469 partitioning, we also followed the approach of previous studies which examined the association  
470 between functional strategies and species niche parameters by using multivariate functional  
471 variables ([Kraft et al. 2015](#), [Muscarella et al. 2016](#), [Pistón et al. 2019](#)). This multivariate trait  
472 approach was generally less predictive than the forward-selected trait approach shown in Fig.  
473 4 (for more details, see Appendix S11: Figure S1 and Figure S2).

474 The overall effect of functional traits on niche breadth variation co-varied with the effect  
475 of niche position (Fig. 4). This suggests that the resource use traits studied here mostly reflect  
476 species edaphic optima and not their range of resource use. It is also worth noting that intra-  
477 specific trait variation may have partly limited the detection of niche-trait association at the  
478 species level ([Zuleta et al. 2022](#)), but we lack enough trait measurements across habitats for  
479 each species to have more accurate insights.

480 Finally, the absence of genus or family-level signal on niche breadth and position  
481 (Appendix S5: Table S1) may suggest that various edaphic niches have evolved multiple times  
482 within many different genera and families, which is consistent with recent reports ([Fine and](#)  
483 [Baraloto 2016](#), [Baraloto et al. 2021](#)).

484 Our results provide further support for the determinant role of soil properties in shaping  
485 tree species assembly in tropical forests ([Russo et al. 2005](#), [Condit et al. 2013](#), [Vleminckx et al.](#)  
486 [2017](#), [Wright et al. 2019](#), [Umaña et al. 2021](#)), while they also provide indirect support to the  
487 hypothesis that the strength of abiotic filtering, here mediated by soil nutrient contents,  
488 determines the degree of species habitat specialization, i.e. to what extent species are confined  
489 to smaller niches because of their costly investments in resource conservation that would  
490 potentially make them less competitive in more fertile habitats. Definitive evidence of  
491 competitive exclusion would further require adding a temporal dimension to these analyses –  
492 i.e. tree demography –, for instance relating tree growth or mortality responses to the interplay

493 of soil, traits, and the functional similarity of the neighborhood (Fortunel et al. 2016, Muledi et  
494 al. 2020, Rozendaal et al. 2020). Such dynamics data unfortunately remain too scarce in the  
495 tropics for accurate characterization of demographic parameters for many species across the  
496 breadth of their distribution ranges, emphasizing the need for continued efforts towards  
497 establishing and monitoring long-term permanent sample plots in the tropics (Blundo et al.  
498 2021, Davies et al. 2021).

499 Here, we did not investigate the possibility that the steep nutrient gradient occurring  
500 across habitat may overlap with a gradient of forest dynamics. Canopy disturbance and forest  
501 turnover rate are likely greater in the most fertile habitats (Baraloto et al. 2011, Baker et al.  
502 2014), with more productive tree communities exhibiting more acquisitive traits (e.g., high  
503 SLA, low leaf thickness...) for soil nutrients and light (Fortunel et al. 2014, Vleminckx et al.  
504 2020, 2021). A greater light extinction profile is also expected on fertile soils (Russo et al.  
505 2012), which may limit the competitiveness of fast-growing species in the understory, although  
506 this effect might be compensated by lower air evaporative demand and thermal constraints  
507 (Vinod et al. 2022) in the more shaded vegetation strata. Accurate gap dynamics history and  
508 light availability data will need to be better studied to further examine how light and soil nutrient  
509 gradients interact to influence niche parameters.

510

### 511 **Implications regarding forest conservation and tree responses to climate change**

512 Species adapted to poor soil conditions likely have large potential edaphic niches  
513 compared to their realized one, as they could in theory thrive on a much wider range of soil  
514 fertilities in the absence of faster-growing competitors, unlike species with higher niche fertility  
515 optimum whose realized and fundamental niches are expected to be more packed. The costly  
516 resource conservation traits displayed by poor-soil specialists are likely to exclude them from  
517 more fertile habitats, explaining the disparities between their realized and fundamental niches.

518 These adaptations might also allow these species to extend their tolerance to other  
519 environmental constraints such as water deficiency (Baraloto et al. 2010), which occurs more  
520 frequently on highly drained white-sands than on terra firme or seasonally flooded soils. This  
521 would potentially render white-sand tree communities more resilient to more prolonged dry  
522 seasons and temperature increases predicted by climate models, predictions that are particularly  
523 threatening in the North-Eastern Amazon (Fortunel et al. 2014, Guevara et al. 2016, Esquivel-  
524 Muelbert et al. 2018, IPCC 2022). These results could also pave the way for developing more  
525 evidence-based forest restoration management plans, for instance by improving the selection of  
526 tree species that would be able to establish in a wide range of environmental conditions. Further  
527 investigations of the interplay of species niche breadth, niche position and functional strategies  
528 for complementary key edaphic and climatic niche dimensions and across different tropical  
529 regions and spatial scales will be urgently needed to better predict how the current context of  
530 rapid environmental changes is likely to affect tropical forest species composition and  
531 associated ecosystem functions.

532

#### 533 4. Acknowledgments

534 JV is a postdoctoral fellow funded by a G. Evelyn Hutchinson Environmental Postdoctoral  
535 Fellowship from the Yale Institute for Biospheric Studies (Yale University, CT, USA). DB was  
536 funded by the European Union's Horizon 2020 research and innovation program under the  
537 Marie Skłodowska-Curie grant agreement No. 895799. This work was supported by  
538 collaborative research grants funded by “Investissement d’Avenir” grants of the ANR  
539 (CEBA:ANR-10-LABX-25-01); by the National Science Foundation (NSF) grant DEB-  
540 0743103/0743800 to CB and PVAF; by ANR Blanc NEBEDIV (Projet ANR-13-BSV7-009)  
541 and an INRAE Package grant to CB; and by NSF DEB 1254214 to PVAF.

542 **5. Author Contributions**

543 C.B. and P.V.A.F. were co-principal investigators for the projects that supported this research.  
544 The collection and identification of tree species was coordinated by C.B and P.V.A.F., with  
545 help of J.E., P.P., N.D., M.R., E.V., I.M., J.G., C.F., E.A., T.P., A.D., J-Y.G., O.V.B., F.D. and  
546 J.V. J.V., C.F., O.V.B. and C.B. led the trait data collection in French Guiana and Peru. J.V.  
547 analyzed the data, with help from D.B. with Bayesian analyses. J.V. led the writing of the  
548 manuscript. C.B., O.V.B., C.F. and D.B. commented on early versions of the manuscript. All  
549 authors contributed to the preparation of the final manuscript.

550 **6. Conflict of Interest Statement**

551 The authors declare no conflict of interest

552 **7. Literature cited**

553 Anderson, M. J. and Legendre, P. 1999. An empirical comparison of permutation methods for  
554 tests of partial regression coefficients in a linear model. – *J. Stat. Comput. Sim.* 62: 271–  
555 303.

556 Asefa, M., Samantha J, W., Cao, M., Xiaoyang, S., Yudi M, L., & Jie, Y. 2022. Above and  
557 belowground plant traits are not consistent in response to drought and competition  
558 treatments. *Annals of Botany*. <https://doi.org/10.1093/aob/mcac108>

559 Baker, T. R., et al. 2014. Fast demographic traits promote high diversification rates of  
560 Amazonian trees. *Ecology Letters* 17:527–536.

561 Baraloto, C. et al. 2010. Decoupled leaf and stem economics in rain forest trees. – *Ecol. Lett.*  
562 13: 1338–1347.

563 Baraloto, C., Rabaud, S., Molto, Q., Blanc, L., Fortunel, C., Herault, B., ... & Fine, P. V. 2011.  
564 Disentangling stand and environmental correlates of aboveground biomass in  
565 Amazonian forests. *Global Change Biology*, 17(8), 2677-2688.



566 Baraloto, C. et al. 2013. Rapid simultaneous estimation of aboveground biomass and tree  
567 diversity across Neotropical forests: a comparison of field inventory methods. –  
568 *Biotropica* 45: 288–298.

569 Baraloto, C., Vleminckx, J., Engel, J., Petronelli, P., Dávila, N., Ríos, M., Valderrama  
570 Sandoval, E. H., Mesones, I., Guevara Andino, J. E., Fortunel, C., Allie, E., Paine, C.  
571 E. T., Dourdain, A., Goret, J.-Y., Valverde-Barrantes, O. J., Draper, F., and Fine, P. V.  
572 A. 2021. Biogeographic history and habitat specialization shape floristic and  
573 phylogenetic composition across Amazonian forests. *Ecological Monographs*  
574 91(4):e01473. 10.1002/ecm.1473

575 Baribault, T.W., Kobe, R.K. & Finley, A.O. (2012). Tropical tree growth is correlated with soil  
576 phosphorus, potassium, and calcium, though not for legumes. *Ecol. Monogr.*, 82, 189–  
577 203.

578 Bauman, D., T. Drouet, M. J. Fortin, and S. Dray. 2018a. Optimizing the choice of a spatial  
579 weighting matrix in eigenvector-based methods. *Ecology* 99:2159–2166.

580 Bauman, D., T. Drouet, S. Dray, and J. Vleminckx. 2018b. Disentangling good from bad  
581 practices in the selection of spatial or phylogenetic eigenvectors. *Ecography* 41:1–12.

582 Blanchet, F. G., P. Legendre, and D. Borcard. 2008. Forward selection of explanatory variables.  
583 *Ecology* 89:2623–2632.

584 Blundo, C., Carilla, J., Grau, R., Malizia, A., Malizia, L., Osinaga-Acosta, O., ... & De Araujo,  
585 R. O. (2021). Taking the pulse of Earth's tropical forests using networks of highly  
586 distributed plots. *Biological Conservation*, 260, 108849.

587 Carscadden, K. A., Emery, N. C., Arnillas, C. A., Cadotte, M. W., Afkhami, M. E., Gravel, D.,  
588 Livingstone, S. W., & Wiens, J. J. (2020). Niche breadth: Causes and consequences for  
589 ecology, evolution, and conservation. *The Quarterly Review of Biology*, 95(3), 179–  
590 214

591 Condit, R., B. M. J. Engelbrecht, D. Pino, R. Perez, and B. L. Turner. 2013. Species  
592 distributions in response to individual soil nutrients and seasonal drought across a  
593 community of tropical trees. *Proceedings of the National Academy of Sciences of the*  
594 *United States of America* 110:5064–5068.

595 Cunha, H. F. V., Andersen, K. M., Lugli, L. F. et al. (2022) Direct evidence for phosphorus  
596 limitation on Amazon forest productivity. *Nature* 608, 558–562.

597 Dauby, G., and O. J. Hardy. 2011. Sampled-based estimation of diversity sensu stricto by  
598 transforming Hurlbert diversities into effective number of species. *Ecography* 34:001–  
599 012.

600 Davies, S. J., Abiem, I., Salim, K. A., Aguilar, S., Allen, D., Alonso, A., ... & Yap, S. L. (2021).  
601 ForestGEO: Understanding forest diversity and dynamics through a global observatory  
602 network. *Biological Conservation*, 253, 108907.

603 Dray, S. et al. 2006. Spatial modelling: a comprehensive framework for principal coordinate  
604 analysis of neighbour matrices (PCNM). – *Ecol. Model.* 196: 483–493.

605 Dray, S., Bauman, D., Blanchet, G., Borcard, D., Clappe, S., Guénard, G., Jombart, T.,  
606 Larocque, G., Legendre, P., Madi, N., Wagner, H.H. (2022) *adespatial: Multivariate*  
607 *Multiscale Spatial Analysis*. R package version 0.3-14. [https://CRAN.R-](https://CRAN.R-project.org/package=adespatial)  
608 [project.org/package=adespatial](https://CRAN.R-project.org/package=adespatial)

609 Dobzhansky T. 1950. Evolution in the tropics. *Am. Sci.* 38:209–21.

610 Dufrière, M., and P. Legendre. 1997. Species assemblages and indicator species: the need for a  
611 flexible asymmetrical approach. *Ecological Monographs* 67:345–366.

612 Esquivel-Muelbert, A., et al. 2018. Compositional response of Amazon forests to climate  
613 change. *Global Change Biology* 25:39–56.

614 Fazayeli, F. et al. 2014. Uncertainty quantified matrix completion using Bayesian hierarchical  
615 matrix factorization. – *Int. Conf. on Machine Learning and Applications (ICMLA)*.

616 Fine, P. V. A., Miller, Z. J., Mesones, I., Irazuzta, S., Appel, H. M., Stevens, M. H., et al. (2006).  
617 The growth-defense trade-off and habitat specialization by plants in Amazonian forests.  
618 Ecology 87, 150–162.

619 Fine, P.V.A., García-Villacorta, R., Pitman, N.C.A., Mesones, I. & Kembel, S.W. (2010).  
620 Floristic Study of the White-Sand Forests of Peru," Annals of the Missouri Botanical  
621 Garden 97(3), 283-305.

622 Fine, P. V. A., Metz, M. R., Lokvam, J., Mesones, I., Ayarza Zuniga, J. M., Lamarre, G. P. A.,  
623 et al. (2013). Insect herbivores, chemical innovation and the evolution of habitat  
624 specialization in Amazonian trees. Ecology 94, 1764–1775.

625 Fine, P. V. A., and C. Baraloto. (2016). Habitat endemism in white-sand forests: insights into  
626 the mechanisms of lineage diversification and community assembly of the Neotropical  
627 flora. Biotropica 48:24–33.

628 Fortunel, C. et al. 2012. Leaf, stem and root tissue strategies across 758 Neotropical tree species.  
629 – Funct. Ecol. 26: 1153–1161.

630 Fortunel, C., C. E. T. Paine, P. V. A. Fine, N. J. B. Kraft, and C. Baraloto. 2014. Environmental  
631 factors predict community functional composition in Amazonian forests. Journal of  
632 Ecology 102:145–155.

633 Fortunel, C., Valencia, R., Wright, S.J., Garwood, N.C. and Kraft, N.J.B. (2016), Functional  
634 trait differences influence neighbourhood interactions in a hyperdiverse Amazonian  
635 forest. Ecol Lett, 19: 1062-1070.

636 Futuyma D. J., Moreno G. 1988. The evolution of ecological specialization. Annual Review of  
637 Ecology, Evolution, and Systematics 19:207–233.

638 Guevara, J. E., et al. 2016. Low phylogenetic beta diversity and geographic neo-endemism in  
639 Amazonian white-sand forests. Biotropica 48:34–46.

640 Gourlet-Fleury, S. et al. 2004. Ecology and management of a neotropical rainforest: lessons  
641 drawn from Paracou, a long-term experimental research site in French Guiana (Gourlet-  
642 Fleury, S. et al., eds). – Elsevier.

643 Hedin LO, Brookshire ENJ, Menge DNL, Barron AR. 2009 The nitrogen paradox in tropical  
644 forest ecosystems. *Annu. Rev. Ecol. Syst.* 40, 613–635

645 Hoorn, C., et al. 2010. Amazonia through time: Andean uplift, climate change, landscape  
646 evolution, and biodiversity. *Science* 330:927–931.

647 Hubbell, S. P. 2001. A unified neutral theory of biodiversity and biogeography. Princeton  
648 University Press, Princeton, New Jersey, USA.

649 Hutchinson, G. E. (1957). Concluding remarks. *Cold Springs Harbor Symposium in*  
650 *Quantitative Biology*, 22, 415–427. <https://doi.org/10.1101/SQB.1957.022.01.039>

651 IPCC, 2022: Climate Change 2022: Impacts, Adaptation and Vulnerability. Contribution of  
652 Working Group II to the Sixth Assessment Report of the Intergovernmental Panel on  
653 Climate Change [H.-O. Pörtner, D.C. Roberts, M. Tignor, E.S. Poloczanska, K.  
654 Mintenbeck, A. Alegría, M. Craig, S. Langsdorf, S. Löschke, V. Möller, A. Okem, B.  
655 Rama (eds.)]. Cambridge University Press. Cambridge University Press, Cambridge,  
656 UK and New York, NY, USA, 3056 pp., doi:10.1017/9781009325844.

657 Kraft, N.J.B., Adler, P.B., Godoy, O., James, E.C., Fuller, S. & Levine, J.M. (2014).  
658 Community assembly, coexistence and the environmental filtering metaphor. *Funct.*  
659 *Ecol.* 29, 592–599.

660 Kraft, N. J., Godoy, O., & Levine, J. M. (2015). Plant functional traits and the multidimensional  
661 nature of species coexistence. *Proceedings of the National Academy of Sciences*,  
662 112(3), 797-802.

663 Laughlin, D.C. (2014). The intrinsic dimensionality of plant traits and its relevance to  
664 community assembly. *J. Ecol.*, 102, 186–193.

665 Le Bagousse-Pinguet, Y., Gross, N., Maestre, F.T., Maire, V., de Bello, F., Fonseca, C.R.,  
666 Kattge, J., Valencia, E., Leps, J. and Liancourt, P. (2017), Testing the environmental  
667 filtering concept in global drylands. *J Ecol*, 105: 1058-1069.  
668 <https://doi.org/10.1111/1365-2745.12735>

669 MacArthur 1969. Patterns of communities in the tropics. *Biological Journal of the Linnean*  
670 *Society* 1: 19-30.

671 McElreath, R. (2020). *Statistical rethinking: A Bayesian course with examples in R and Stan*.  
672 Chapman and Hall/CRC.

673 McGill, B.J., Enquist, B.J., Weiher, E. & Westoby, M. (2006) Rebuilding community ecology  
674 from functional traits. *Trends in Ecology & Evolution*, 21, 178–185.

675 Malanson, G.P., Westman, W.E. & Yan, Y.L. (1992) Realized versus fundamental niche  
676 functions in a model of chaparral response to climatic change. *Ecological Modelling*,  
677 64, 261–277.

678 Muledi, J., Bauman, D., Jacobs, A., Meerts, P., Shutcha, M., & Drouet, T. (2020). Tree growth,  
679 recruitment, and survival in a tropical dry woodland: The importance of soil and  
680 functional identity of the neighbourhood. *Forest ecology and management*, 460, 117894.

681 Muscarella, R., & Uriarte, M. (2016). Do community-weighted mean functional traits reflect  
682 optimal strategies?. *Proceedings of the Royal Society B: Biological Sciences*,  
683 283(1827), 20152434.

684 Phillips, O. L., R. Vásquez Martínez, P. Núñez Vargas, A. Lorenzo Monteagudo, M.-E. Chuspe  
685 Zans, W. Galiano Sánchez, A. Peña Cruz, M. Timaná, M. Yli-Halla, and S. Rose. 2003.  
686 Efficient plot-based floristic assessment of tropical forests. *Journal of Tropical Ecology*  
687 19:629–645.

688 Pianka ER. 1966. Latitudinal gradients in species diversity: a review of the concepts. *Am. Nat.*  
689 100:33–46.

690 Pinho, B.X., Melo, F.P.L., Arroyo-Rodríguez, V., Pierce, S., Lohbeck, M., Tabarelli, M. Soil-  
691 mediated filtering organizes tree assemblages in regenerating tropical forests. *J Ecol.*  
692 2017; 00: 1– 11. <https://doi.org/10.1111/1365-2745.12843>

693 Pistón, N., de Bello, F., Dias, A.T.C., et al. (2019) Multidimensional ecological analyses  
694 demonstrate how interactions between functional traits shape fitness and life history  
695 strategies. *Journal of Ecology* 107: 2317–2328. [https://doi.org/10.1111/1365-](https://doi.org/10.1111/1365-2745.13190)  
696 [2745.13190](https://doi.org/10.1111/1365-2745.13190)

697 Poorter, L., Castilho, C.V., Schiatti, J., Oliveira, R.S. and Costa, F.R.C. (2018), Can traits  
698 predict individual growth performance? A test in a hyperdiverse tropical forest. *New*  
699 *Phytol*, 219: 109-121. doi:10.1111/nph.15206

700 Quesada, C. A., Lloyd, J., Schwarz, M., Patiño, S., Baker, T. R., Czimczik, C., ... & Paiva, R.  
701 (2010). Variations in chemical and physical properties of Amazon forest soils in relation  
702 to their genesis. *Biogeosciences*, 7(5), 1515–1541.

703 R Development Core Team. 2022. R: a language and environment for statistical computing. R  
704 Foundation for Statistical Computing, Vienna, Austria. [www.R-project.org](http://www.R-project.org)

705 Reich, P. B. 2014. The world-wide ‘fast–slow’ plant economics spectrum: a traits manifesto. –  
706 *J. Ecol.* 102: 275–301.

707 Roughgarden J. 1974. Niche width: biogeographic patterns among *Anolis* lizard populations.  
708 *American Naturalist* 108:429–442.

709 Rozendaal, D. M., Phillips, O. L., Lewis, S. L., Affum-Baffoe, K., Alvarez-Davila, E., Andrade,  
710 A., ... & Vanderwel, M. C. (2020). Competition influences tree growth, but not  
711 mortality, across environmental gradients in Amazonia and tropical Africa. *Ecology*,  
712 101(7), e03052.

713 Russo, S.E., Davies, S.J., King, D.A. & Tan, S. (2005) Soil-related performance variation and  
714 distributions of tree species in a Bornean Rain Forest. *Journal of Ecology*, 93, 879–889.

715 Russo, S., Zhang, L., & Tan, S. (2012). Covariation between understorey light environments  
716 and soil resources in Bornean mixed dipterocarp rain forest. *Journal of Tropical*  
717 *Ecology*, 28(1), 33-44. doi:10.1017/S0266467411000538

718 Santiago LS, Wright SJ, Harms KE, Yavitt JB, Korine C, Garcia MN, Turner BL (2012)  
719 Tropical tree seedling growth responses to nitrogen, phosphorus and potassium addition.  
720 *J Ecol* 100:309–316.

721 Sexton, J. P., Montiel, J., Shay, J. E., Stephens, M. R. and Slatyer, R. A. (2017) Evolution of  
722 Ecological Niche Breadth. *Annual Review of Ecology, Evolution, and Systematics* 2017  
723 48:1, 183-206.

724 Sheth, S. N., Morueta-Holme, N. & Angert, A. L. Determinants of geographic range size in  
725 plants. *New Phytologist* 226: 650–665.

726 Steidinger, B. (2015). Qualitative differences in tree species distributions along soil chemical  
727 gradients give clues to the mechanisms of specialization: why boron may be the most  
728 important soil nutrient at Barro Colorado Island. *New Phytologist*, 27, 206(3):895-899.

729 Sultan S. E., Wilczek A. M., Hann S. D., Brosi B. J. 1998. Contrasting ecological breadth of  
730 co-occurring annual *Polygonum* species. *Journal of Ecology* 86:363–383.

731 Taylor, L. (1961) Aggregation, Variance and the Mean. *Nature* 189, 732–735.

732 Treurnicht, M., Pagel, J., Tonnabel, J., Esler, K.J., Slingsby, J.A. & Schurr, F.M. (2019)  
733 Functional traits explain the Hutchinsonian niches of plant species. *Global Ecol*  
734 *Biogeogr.* 29: 534–545.

735 Turner, B., Brenes-Arguedas, T. & Condit, R. Pervasive phosphorus limitation of tree species  
736 but not communities in tropical forests. *Nature* 555, 367–370 (2018).  
737 <https://doi.org/10.1038/nature25789>

738 Umaña, MN, Condit, R, Pérez, R, Turner, BL, Wright, SJ, Comita, LS. (2021) Shifts in  
739 taxonomic and functional composition of trees along rainfall and phosphorus gradients  
740 in central Panama. *J Ecol.* 109: 51– 61. <https://doi.org/10.1111/1365-2745.13442>

741 Valverde-Barrantes, O. J. et al. 2017. A worldview of root traits: the influence of ancestry,  
742 growth form, climate and mycorrhizal association on the functional trait variation of  
743 fine-root tissues in seed plants. – *New Phytol.* 215: 1562–1573.

744 Van Breugel, M., D. Craven, H. Ran Lai, M. Baillon, B. L. Turner, J. S. Hall. 2019. Soil  
745 nutrients and dispersal limitation shape compositional variation in secondary tropical  
746 forests across multiple scales. *Journal of Ecology* 107:566–581.

747 Vinod, N., Slot, M., McGregor, I.R., Ordway, E.M., Smith, M.N., Taylor, T.C., et al. (2022).  
748 Thermal sensitivity across forest vertical profiles: patterns, mechanisms, and ecological  
749 implications. *New Phytol.*, 237, 22–47.

750 Vleminckx, J., T. Drouet, C. Amani, J. Lisingo, J. Lejoly, and O. J. Hardy. 2015. Impact of  
751 fine-scale edaphic heterogeneity on tree species assembly in a central African rainforest.  
752 *Journal of Vegetation Science* 26:134–144.

753 Vleminckx, J. et al. 2017. The influence of spatially structured soil properties on tree  
754 community assemblages at a landscape scale in the tropical forests of southern  
755 Cameroon. – *J. Ecol.* 105: 354–366.

756 Vleminckx, J, Bauman, D, Demanet, M, Hardy, OJ, Doucet, J-L, Drouet, T. Past human  
757 disturbances and soil fertility both influence the distribution of light-demanding tree  
758 species in a Central African tropical forest. *J Veg Sci.* 2020; 31: 440– 453.  
759 <https://doi.org/10.1111/jvs.12861>

760 Vleminckx J, Fortunel C, Valverde-Barranted O, Paine CET, Engel J, Petronelli P, Dourdain  
761 AK, Guevara JE, Bérroujon S & Baraloto C (2021) Resolving whole-plant economics



762 from leaf, stem and root traits of 1467 Amazonian tree species. *Oikos*, 130(7): 1193-  
763 1208.

764 Vleminckx et al. (2023). Niche breadth of Amazonian trees increases with niche optimum  
765 across broad edaphic gradients: Supplementary information provided through the  
766 Harvard Dataverse repository: <https://doi.org/10.7910/DVN/VWAJYR>

767 Wagner, H. H., and S. Dray. 2015. Generating spatially constrained null models for irregularly  
768 spaced data using Moran spectral randomization methods. *Methods in Ecology &*  
769 *Evolution* 6:1169–1178.

770 Walker, T. W. & Syers, J. K. The fate of phosphorus during pedogenesis. *Geoderma* 15, 1–19  
771 (1976).

772 Wright SJ, Yavitt JB, Wurzburger N, Turner BI, Tanner EVJ, Sayer EJ, Santiago LS, Kaspari  
773 M, Hedin LO, Harms KE, Garcia MN, Corre MD (2011) Potassium, phosphorus, or  
774 nitrogen limit root allocation, tree growth, or litter production in a lowland tropical  
775 forest. *Ecology* 92:1616–1625. <https://doi.org/10.1890/10-1558.1>

776 Wright, S. J. 2019. Plant responses to nutrient addition experiments conducted in tropical  
777 forests. *Ecological Monographs* 89( 4):e01382. 10.1002/ecm.1382

778 Wurzburger N, Wright SJ. 2015. Fine-root responses to fertilization reveal multiple nutrient  
779 limitation in a lowland tropical forest. *Ecology* 96: 2137–2146.

780 Zuquim, G., Costa, F.R.C., Tuomisto, H. et al. The importance of soils in predicting the future  
781 of plant habitat suitability in a tropical forest. *Plant Soil* 450, 151–170 (2020).  
782 <https://doi.org/10.1007/s11104-018-03915-9>

783 Zuleta, D., Muller-Landau, H. C., Duque, A., Caro, N., Cardenas, D., Castaño, N., León-Peláez,  
784 J. D., & Feeley, K. J. (2022). Interspecific and intraspecific variation of tree branch, leaf  
785 and stomatal traits in relation to topography in an aseasonal Amazon forest. *Functional*  
786 *Ecology*, 36, 2955– 2968. <https://doi.org/10.1111/1365-2435.14199>

787

788

790 **Table 1.** Summary of key descriptors of study regions, subregions and habitats. NrP = Number  
 791 of plots; AR = Altitudinal Range (in m); MAR = Mean Annual Rainfall (in mm); MAT = Mean  
 792 Annual Temperature (in °C). NrSp = mean number of species per plot; ENS<sub>2</sub> = mean (calculated  
 793 at the plot level) Effective Number of Species expected from 1000 random samplings (with  
 794 replacement) of two individuals. The three last lines of each region represent the same  
 795 information for each habitat. Numbers in parenthesis correspond to the standard deviation of  
 796 the mean.

	NrP	AR	MAR	MAT	NrSp	ENS <sub>2</sub>
<b><i>French Guiana</i></b>	64	42-529	2157- 3129	23.0- 26.6	80.3 (3.6)	48.6 (5.2)
<b><i>Saül-Limonade</i></b>	12	196-253	2421	24.6	66.1 (4.2)	24.4 (4.5)
<b><i>Trinité</i></b>	6	126-320	2671	25.1	112.8 (11.7)	77.8 (14.0)
<b><i>Itoupé</i></b>	3	521-529	2530	23.0	79.7 (6.9)	30.1 (7.0)
<b><i>Mitaraka</i></b>	9	317-347	2157	24.9	70.8 (10.7)	66.1 (17.2)
<b><i>Laussat</i></b>	10	49-57	2402	26.2	74.1 (3.7)	28.0 (4.0)
<b><i>Nouragues</i></b>	8	108-345	3328	24.8	86.9 (14.0)	68.0 (20.5)
<b><i>Petite montagne Tortue</i></b>	9	47-136	3729	25.4	95.0 (10.5)	66.3 (17.0)
<b><i>Centre Spatial Guyanais</i></b>	4	43-63	2932	25.8	76.0 (9.2)	25.3 (5.1)
<b><i>Kaw</i></b>	2	254-282	3720	24.5	96.0 (6.0)	73.9 (18.5)
<b><i>Suriname</i></b>	2	196-229	2241	26.6	38.5 (3.5)	10.1 (6.3)
<b><i>Terra Firme</i></b>	20	45-347	2775	25.2	95.5 (4.4)	70.8 (7.6)
<b><i>Seasonally Flooded</i></b>	35	43-529	2723	24.9	64.7 (5.2)	24.5 (4.2)
<b><i>White Sand</i></b>	10	39-345	2908	25.7	59.5 (5.6)	21.1 (4.7)
<b><i>Peru</i></b>	38	95-173	2405- 2750	26.3- 26.7	101.4 (4.99)	61.2 (6.7)
<b><i>Morona</i></b>	6	143-173	2405	26.7	108.2 (6.0)	89.4 (17.2)
<b><i>North Loreto</i></b>	18	105-149	2750	26.3	101.6 (8.7)	59.9 (10.5)
<b><i>South Loreto</i></b>	14	95-139	2499	26.8	98.3 (7.5)	50.7 (9.0)
<b><i>Terra Firme</i></b>	11	95-158	2597	26.6	128.8 (5.6)	101.6 (9.6)
<b><i>Seasonally Flooded</i></b>	13	106-156	2636	26.5	87.7 (6.1)	53.4 (9.2)
<b><i>White Sand</i></b>	14	106-173	2625	26.6	86.7 (7.8)	29.8 (5.0)

799 **Table 2.** Mean ( $\pm$  standard deviation) of each soil variable in each habitat (SF = Seasonally  
800 Flooded; TF = Terra Firme; WS = White-Sand) and each study region (French Guiana and  
801 Peru).

<i>Habitat</i>	French Guiana			Peru		
	SF	TF	WS	SF	TF	WS
<i>TN (%)</i>	2.29 (3.25)	1.65 (1.35)	0.17 (0.22)	0.23 (0.09)	0.14 (0.05)	0.07 (0.06)
<i>Avail. P (mg/kg)</i>	10.78 (15.51)	5.07 (5.81)	3.67 (4.11)	7.4 (5.75)	2.25 (1.54)	8.4 (8.01)
<i>Ca (mg/kg)</i>	1.26 (2.37)	0.53 (1.02)	0.16 (0.17)	5.96 (7.23)	0.84 (2.58)	0.04 (0.03)
<i>Mg (mg/kg)</i>	0.81 (0.92)	0.32 (0.31)	0.22 (0.24)	1.35 (1.45)	0.31 (0.6)	0.05 (0.04)
<i>K (mg/kg)</i>	0.13 (0.11)	0.1 (0.04)	0.05 (0.05)	0.18 (0.07)	0.06 (0.02)	0.06 (0.03)

802

803

804

805 10. Figure captions

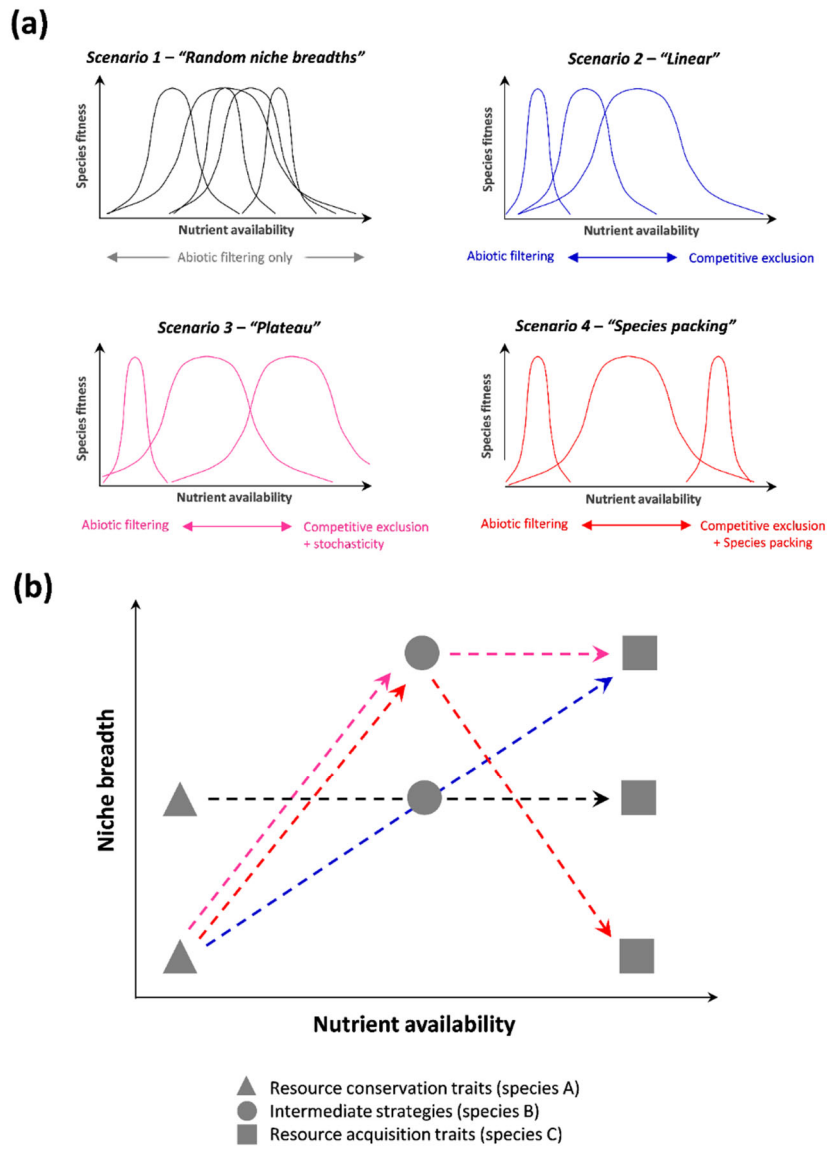
806 **Figure.1** (a) Hypothetical scenarios describing species frequency distributions (realized niches)  
807 along a gradient of increasing soil nutrient availability, using Gaussian curves for simplicity.  
808 (b) Translation of these scenarios into niche breadth – niche positions graphs, showing species  
809 and predicted functional strategies with symbols.

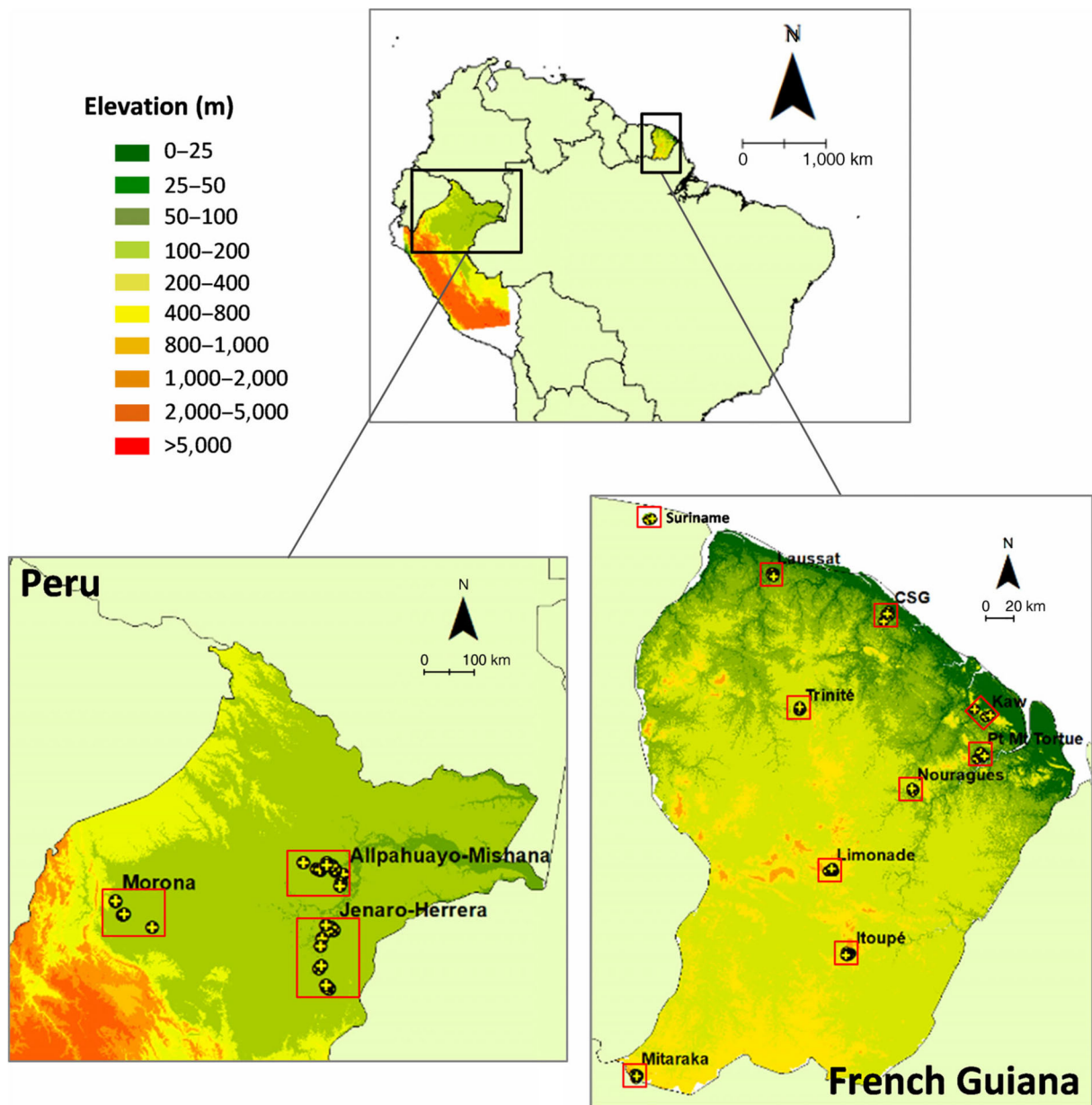
810 **Figure 2.** Geographical distribution of the 13 subregions in the Amazon (red rectangles),  
811 showing the position of the plots (yellow cross symbols) within the two study regions (Peru and  
812 French Guiana).

813 **Figure 3.** Projection of species and soil variables on axes 1-2 of a principal component analysis  
814 (PCA) performed on niche breadth (a) and niche position (b) values. The grey rectangle that  
815 connects both PCA graphs shows the Procrustes correlation quantifying the matching of soil  
816 variables and species projections between the two PCAs ( $P \leq 0.001$ ; MSR test). The histograms  
817 show the relative eigenvalues of each PCA axis (only the first axis in each PCA expressed more  
818 variation than expected under a broken stick model). Symbols in the graphs indicate whether  
819 species are significantly indicative of one of the three habitats (seasonally flooded, terra firme,  
820 or white-sand specialist) or not (generalist). Tables at the bottom show the Pearson correlations  
821 of niche breadth (c) and niche position (d) values among soil variables. The significant  
822 correlations ( $t$ -test of Pearson's moment correlation) are indicated in blue (grey values were not  
823 significant).

824 **Figure 4.** Niche breadth–niche position relationship among the 246 species, for each of four  
825 soil nutrients. Values indicated along x and y axes corresponded to back-transformed niche  
826 breadth and niche position values, respectively. Traits significantly explained niche breadth  
827 variation for N, Ca, and P. For these three nutrients, the Venn diagram on the right of the niche  
828 breadth-position graph shows the relative linear contribution (adjusted  $R^2$  from a variation  
829 partitioning analysis) of niche position alone, traits alone, and the joint influence of niche

830 position and traits. Individual traits that significantly explained niche breadth variation (i.e., the  
831 traits selected from a forward selection procedure, which was performed if the overall effect of  
832 traits was significant when using the MSR testing procedure; see methods for details) were  
833 indicated on the right of the Venn diagram, with colors indicating whether correlations were  
834 positive (blue) or negative (red) between niche breadth and the trait. Symbols indicate whether  
835 species are significantly indicative (significant indval) of one of the three habitats (see the  
836 legend panel at the bottom right of the figure). The two grey regions in each graph represent  
837 two different 95% Bayesian plausible intervals for predicted niche breadth values. The narrow  
838 interval shows the distribution of estimated mean niche breadth values, while the wide interval  
839 corresponds to the region in which the non-linear model expects to find 95% of actual niche  
840 breadth values at each niche position value. The equation in each graph shows the median of  
841 the Bayesian credibility interval for the linear and quadratic coefficients and the intercept.  
842 Significant coefficients (i.e., at least 95% of estimated posterior coefficient values being  
843 positive) were emphasized in bold. No significant quadratic effects were found for traits.  
844 Asterisks in the Venn diagrams indicate significant adjusted  $R^2$  values quantifying the relative  
845 effect of niche position alone, traits alone and the co-variation of both niche position and traits,  
846 according to the MSR testing procedure (see methods): \*\*\* $P \leq 0.001$ ; \*\* $P \leq 0.01$ ; \* $P \leq 0.05$ .  
847





855

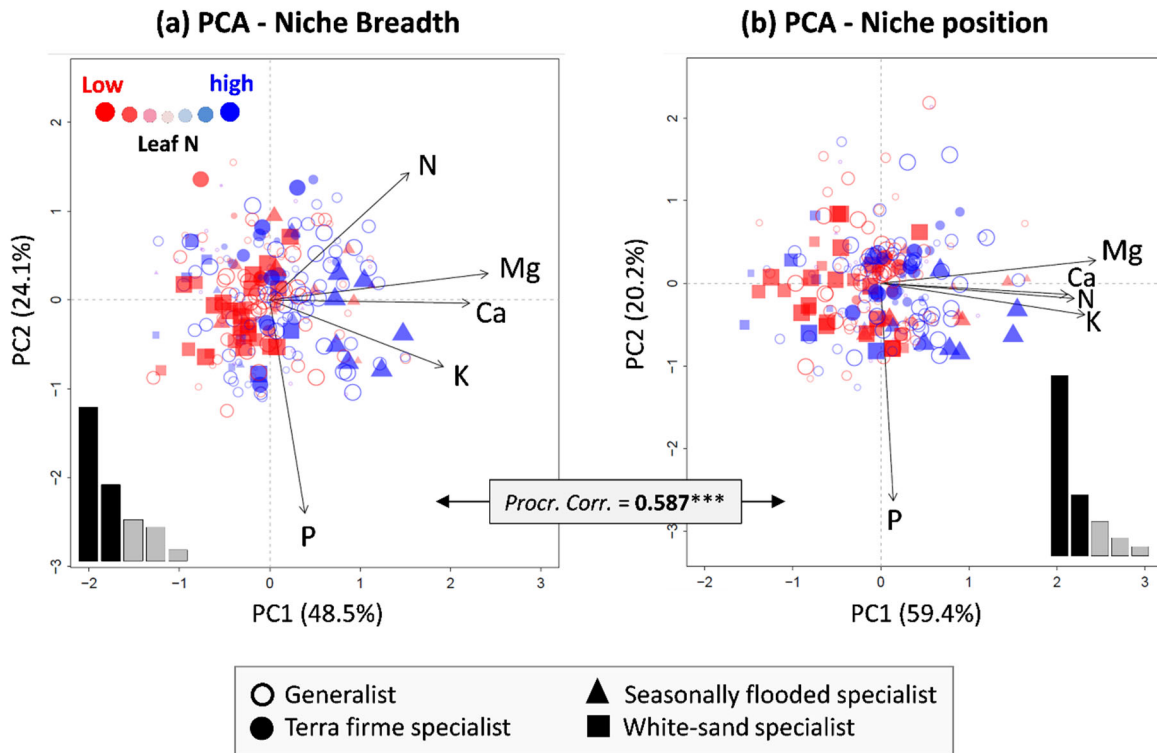
856 **Figure 2.**

857

858

859





(c) Niche breath correlations

	N	Ca	Mg	K
Ca	0.34			
Mg	0.45	0.77		
K	0.27	0.38	0.55	
P	-0.20	0.12	-0.01	0.23

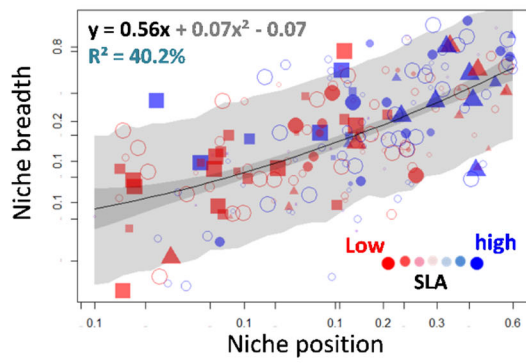
(d) Niche position correlations

	N	Ca	Mg	K
Ca	0.50			
Mg	0.64	0.74		
K	0.72	0.54	0.75	
P	0.09	0.11	-0.03	0.17

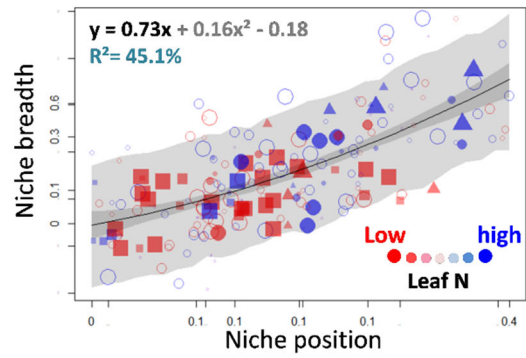
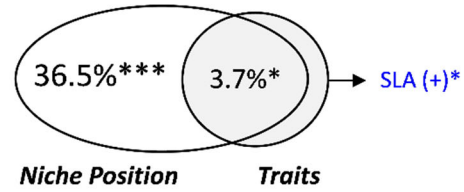
860

861 **Figure 3.**

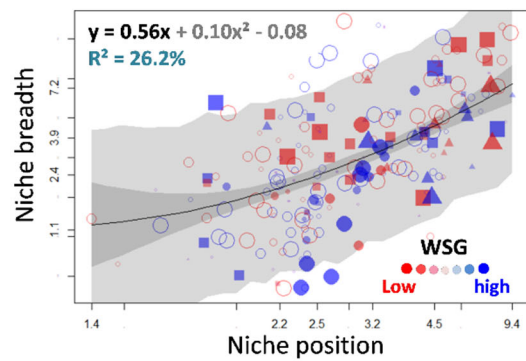
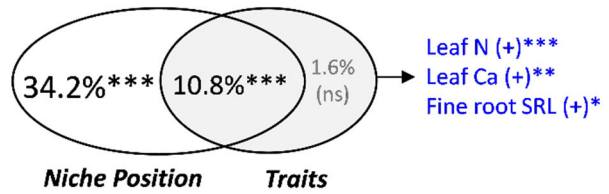
862



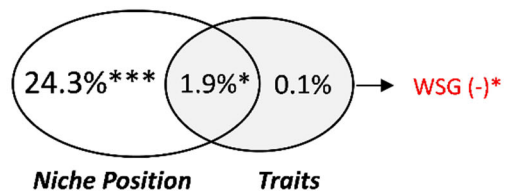
### Soil N content



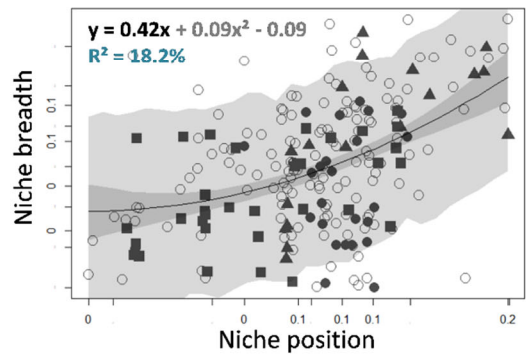
### Soil Ca content



### Soil P content



### Soil K content



- Generalist
- ▲ Seasonally flooded specialist
- Terra firme specialist
- White-sand specialist

863

864 **Figure 4.**

865

866